Numerical Analysis of Laterally Loaded Piles: Foundation of Tracker Systems

Naloan C. Sampa[1], Gabryel G. Soares[1], Gracieli Dienstmann[1]

[1]*Dept. of Civil Engineering, Federal University of Santa Catarina*
João Pio Duarte da Silva - 205, 88040-900, Santa Catarina, Brazil
naloan.sampa@ufsc.br, gabryel.soares@grad.ufsc.br, g.dienstmann@ufsc.br

Abstract. This paper presents and discusses a numerical study of the laterally loaded pile. The numerical analysis considers two setups, with different excentricities and points to measure horizontal displacements. Results highlight the effects of eccentricity and displacement measurement points on load-displacement curves. For practical application, some quantities and considerations about lateral load and horizontal displacements in SLS and ULS are presented and discussed. The conclusions presented in this paper can be of great importance for planning lateral load tests and interpreting their results in solar photovoltaic parks.

Keywords: numerical analysis, foundation, steel piles, lateral load tests, tracker systems.

1 Introduction

Currently, solar energy occupies approximately 1.4% of the total renewable energy in Brazil and presents the greatest potential for growth due to the favorable environmental conditions, an increase in demand for energy and the development of the industry. Allied to this, there is the need to diversify the electric matrix and reduce the emission of greenhouse gases to values compatible with those promised in international agreements, aiming at the preservation of the environment.

The solar energy is generated through photovoltaic modules fixed on trackers that work as support structures. Trackers are devices that guide the solar photovoltaic modules toward the sun and are fixed to the top of the steel piles, and these piles are designed to receive and resist the wind loads acting on the photovoltaic modules and then transmit them to the soil. For this reason, the measurement of the wind loads is usually obtained through wind tunnels tests according to the operation of the trackers, varying the inclination of the modules. The combination of these loads is recommended by codes for the analysis of the structural deformation of the components and support structures of photovoltaic tracker systems, and the design of steel piles through analytical or numerical methods.

The wind loads acting on the photovoltaic modules have been investigated and reported by Mohapatra [1], Silva [2], Kaabia et al. [3] and Wu et al. [4]. Wu et al. [4] investigated both the velocity distribution and wind load in order to quantify the effects of elevation angle and wind speed on the structural strength of trackers. Kaabia et al. [3] evaluated the full-scale wind response of a concentrated photovoltaic prototype and correlate it with wind measurements made near the solar structure.

In fact, the tracker system is relatively light and the intense action of wind loads tries to lift it, thus generating pullout load on the pile. The length of steel piles in earth, designed to resist these loads, is no more than 4m, thus requiring a good investigation of the first layers of soil. Furthermore, the performance of the piles is usually analyzed through lateral and axial compression and tension static load tests.

Although compression capacity is not of paramount importance in the design of the foundation of tracker systems, its estimation has been made based on Aoki-Velloso's [5] and Décourt-Quaresma's [6] methods. For the calculation of tension (uplift) capacity, Grenoble's method has often been used because it is comprehensive and

works for virtually all types of foundations. Regarding lateral loads, the interaction mechanisms between the soil and laterally loaded piles have been extensively discussed by Reese et al. [7], Broms [8 and 9], Matlock and Reese [10] and others. For cohesive and cohesionless soils, Broms [8 and 9] have proposed equations and charts to estimate directly the lateral deflection at the ground surface and lateral capacity for long, short, unrestrained, and restrained piles. In addition to the theoretical studies, Desai and Appel [11], Desai and Kuppusamy [12], Khodair and Abdel-Mohti [13], and others have discussed the interaction mechanisms through numerical analysis.

Most of the numerical studies in this field have been applied intensively to investigate the load transfer and interaction mechanisms between soil and long piles under different loading conditions. On the other end, there are still few numerical studies on short piles commonly designed and installed in solar photovoltaic parks. This paper analyses, through the numerical model, the effects of eccentricity and the measuring point of horizontal displacement on the behavior of the load-displacement curves in order to clarify some questions regarding the planning and interpretation of the results of lateral load tests on short steel piles.

2 Field Tests and Problem Definition

Around 170,240 piles (60% direct damping and 40% micropiles) are planned to be installed in a solar photovoltaic park area of approximately 754 hectares. The geotechnical investigation in this area involves physical characterization tests, CBR, inspection shaft, SPT, DPSH, and Pull-Out Tests (POTs). Pull-Out Tests comprise compression, tension and lateral load test with or without loading and unloading cycles. The plan of POTs depends on the regional wind conditions. Generally, more than one type of loading is performed on the same pile of profiles I, C or Omega. When this is not possible, only the lateral load tests are carried out. In addition, depending on the soil resistance, the installation of the piles may be direct damping, pre-drilling or micropile. Direct damping is simulated in this paper as it is the most common installation type.

The height of the horizontal load application point (eccentricity - e) is associated with the configuration of tracker systems, varying between 0.4 m and 2.0 m. The design load applied to the piles is specified by the trackers and photovoltaic modules suppliers based on the structural analysis of these products. In contrast, the load application time and the number of loading and unloading cycles procedures are based on ASTM D3966.07 and ASTM D3689.07 standards. Due to the difficulty of measuring displacement on the ground surface, the horizontal displacement is measured approximately at point *m* located 10 cm above the ground surface through a dial height gauge comparator. This horizontal displacement is greater than the horizontal displacement at the ground surface, and this difference (y_{res}) depends on the pile and soil characteristics, as well as the eccentricity. As a consequence, it is important to investigate numerically this problem and quantify the magnitude of this difference for different setups in order to correctly interpret the experimental load-displacement curves.

To analyze this problem, two cases of laterally loaded piles (Fig. 1) were modeled in Abaqus. The first case simulates a pile under lateral load, with the bottom of the free section of the pile being crimped, while the second one simulates the real condition of the lateral load test on piles driven into the soil. Both cases consider I profiles (W150 × 13.0), eccentricities (e) of 1.5 m, 1.2 m, 0.9 m, 0.6 m and 0.3 m, and free section length of 1.5 m. In the second case, the length of the pile in earth (L) is equal to 3.3 m.

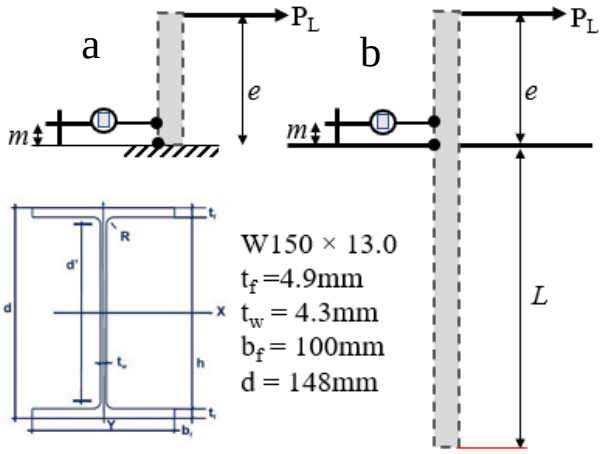

Figure 1. A schematic representation of lateral loading test - a) 1st case and b) 2nd case

3 Finite Element Model

Three-dimensional FE analyses are carried out to simulate lateral load tests, using the commercially finite element software Abaqus. Due to the symmetry condition of the laterally loaded piles, a half soil domain of length 6 m, width 2.1 m and depth 7.5 m is modeled. This domain is large enough to avoid any significant boundary effects on calculated displacement, deformation and load. Refined meshes are used in regions surrounding the pile, where higher stress and strain concentrations are expected. The large domain and refined meshes allow us not to perform the sensitivity analysis. Figures 3 and 4 show the typical FE mesh of the first and second cases, respectively. The pile is modeled with the same cross-section as those of commercial I profiles (W 150 × 13.0) presented in Fig. 1. Concerning the boundary conditions, vertical displacement is allowed on all sides of the soil domain except at the bottom, where all displacements are restrained. The vertical plane of symmetry is restrained from any displacement perpendicular to it. The other sides of the soil domain are restrained from any lateral displacement through the roller supports. For the first case, the vertical plane of symmetry is restrained from any displacement perpendicular to it, while the bottom is restrained from any movement or rotation.

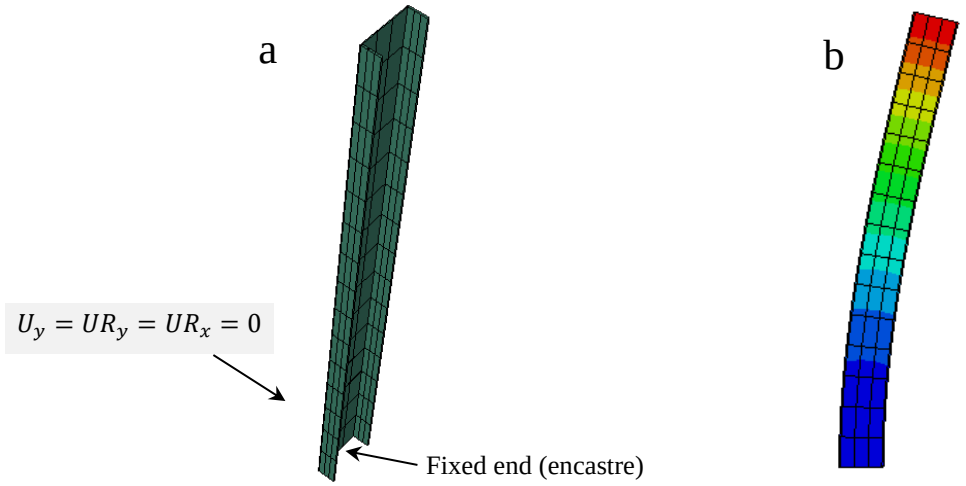

Figure 2. a) Discretized FE domain and boundary conditions, b) deformed shape of the laterally loaded pile (2nd case)

The pile is modeled as a rigid body and also as elastic-perfectly plastic material with Young's modulus equated to 210 GPa and Poisson's ratio equated to 0.2. The soil is defined as elastoplastic material obeying the Mohr-Coulomb failure criterion. The soil properties are calculated from the laboratory tests and SPT. The internal frictional angle is 37º, the dilatancy angle is 6º, the cohesion of 12.5 kPa, the bulk unit weight is 19 kN/m³, Young's modulus is 40 MPa and Poisson's ratio is 0.3. Both materials, soil and pile, are modeled using the C3D8R solid homogeneous elements, which is an 8-noded linear brick element with reduced integration and hourglass control to overcome shear locking.

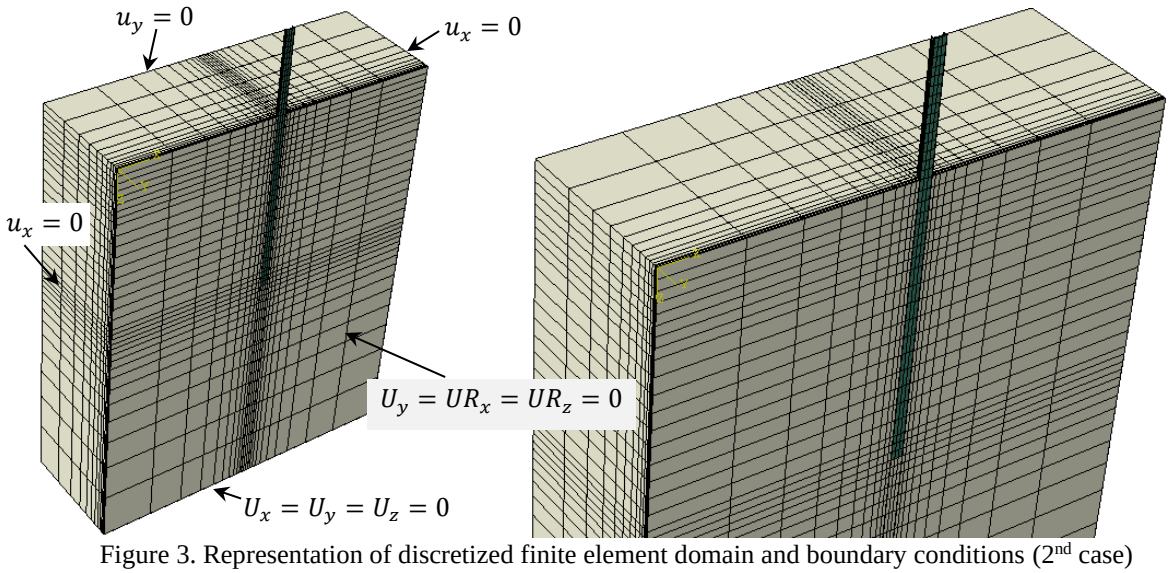

Figure 3. Representation of discretized finite element domain and boundary conditions (2nd case)

The contact surfaces between the pile and the soil are discretized using the surface-to-surface contact technique with the master-slave contact algorithm. Hard contact is assumed as the normal contact of all interfaces, and the shear contact between soil and pile is modeled as the Coulomb friction model. Among several expressions available to calculate the friction coefficient of the pile-soil interface, the expression $\left(\mu = \tan\left(\frac{2}{3}\phi'\right)\right)$ is adopted, where μ is the friction coefficient and ϕ' is the internal friction angle of the soil.

To investigate the influence of the eccentricity in load-displacement curves, loads are applied at 5 different eccentricities, as mentioned earlier. For the second case, numerical analyses were performed in three steps: a) body force option was used to establish the initial self-weight stress field on the soil domain, considering K_0 equal to 0.40 ($= 1 - \sin\phi'$), b) installation of the pile and c) application of the lateral load by a displacement boundary condition at the eccentricity. The maximum displacement applied was 0.1 m, based on the steel pile width ($b_f =$ 10 cm). Horizontal displacements are collected at two points – 1) point *m* and 2) point located on the ground surface.

4 Results and Discussion

To validate the numerical model, Fig. 4 compares the load-displacement curve of the numerical analysis with the experimental results for laterally loaded piles at e = 1.2 m. Although the experimental tests were carried out with controlled lateral loads, unlike the controlled displacement boundary condition adopted in numerical modeling, the superposition of the results shows the reliability of the numerical model from a practical point of view and allows concluding that the model can be used to perform the analyses presented and discussed below.

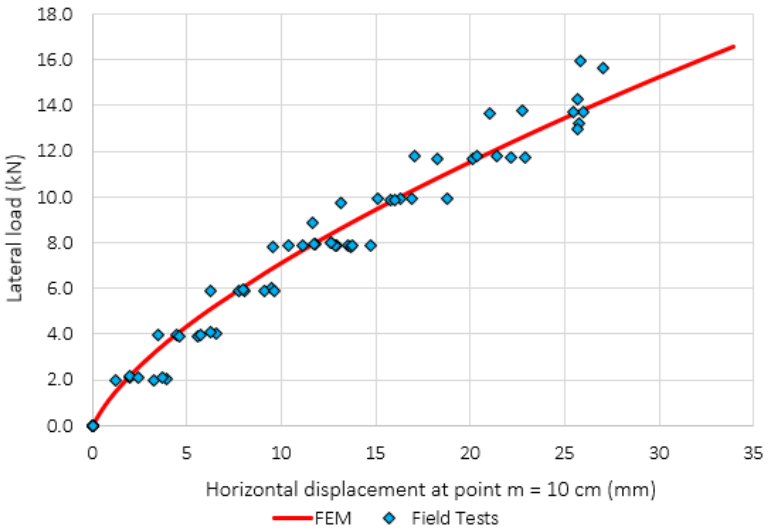

Figure 4. Comparison of FEM with experimental results.

Figures 5a and 5b show horizontal load-displacement curves measured at the ground surface and point *m*, respectively, for different eccentricities. Vertical lines represented in the graph indicate maximum displacements for Serviceability Limit State (10 mm) and Ultimate Limit State (25 mm), while horizontal lines highlight design load (11.6 kN) and a surcharge of 150% and 250% of the design load. These values are used as acceptance criteria for the lateral load test results. As expected, in both figures, an increase in horizontal displacement is observed with increasing eccentricity, for the same lateral load, and larger values of horizontal displacements are found in Fig. 5b.

Considering that the performance analysis of lateral load tests on piles of solar photovoltaic parks stipulates a maximum horizontal displacement of 10 mm for a design load of 11.6 kN, both figures show that this criterion tends to be satisfied for eccentricities smaller than 0.6 m. The same trend is observed when analyzing the criterion of 25 mm for 150% of the design load. None of the eccentricities greater than 0 cm meets the criterion of 25 mm for 250% of the design load. In addition to eccentricity, it is also expected that this behavior is dependent on soil and pile characteristics.

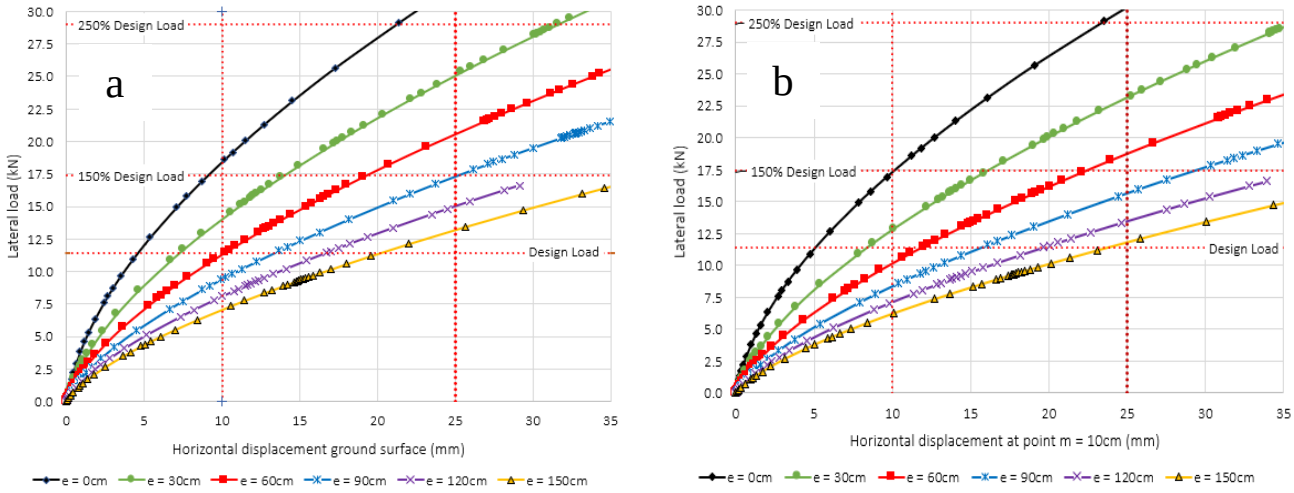

Figure 5. Load-displacement curves: a) horizontal displacement measured at the ground surface, b) horizontal displacement measured at point m.

Figure 6a shows the variation of the pile deflection (minimum horizontal displacement) at point *m* with the horizontal displacement at eccentricities, considering the first case. It is possible to observe from this figure that the displacements at point *m* do not exceed 2 mm when the displacement at eccentricities greater than or equal to 0.6 m is smaller than 30 cm. These deflection values correspond to the minimum required to correct the horizontal displacement of piles when analyses require displacements measured on the ground surface. Figure 6b shows the same relationship for the second case, where larger values of horizontal displacements are observed at point *m*. Considering that it is difficult in field to measure horizontal displacement on the ground surface, it is important to take into account the pile deflection and the soil stiffness in order to correct the load-displacement curves for the ground surface condition. This correction can validate test results that would fail for excessive horizontal displacement.

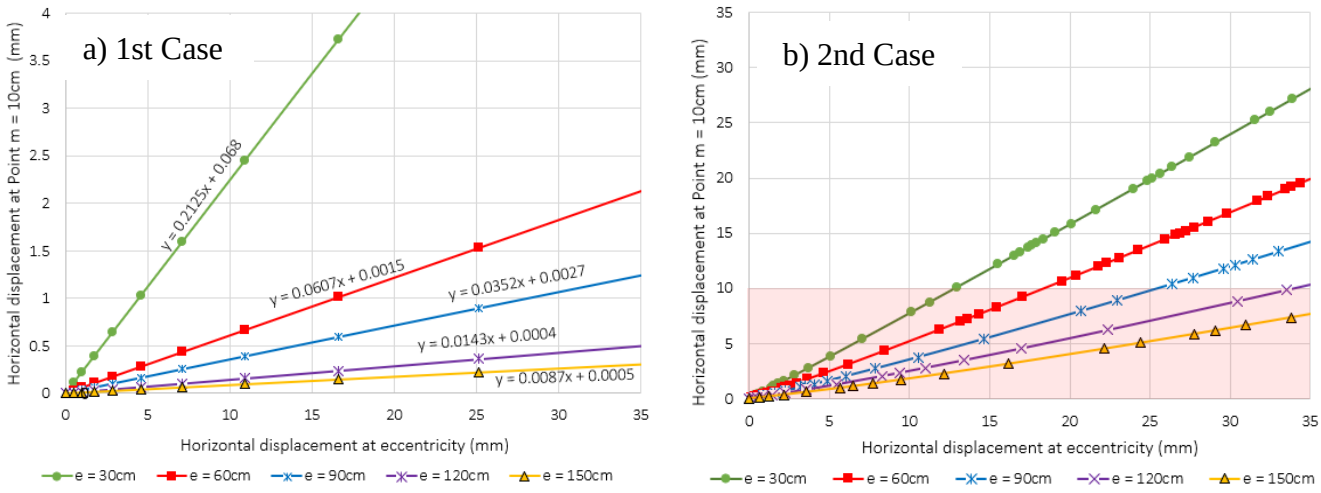

Figure 6. Relationship between horizontal displacements measured at point m and eccentricity: a) results of the first case, b) results of the second case.

Taking into account the design load of 11.6kN, Fig. 7a shows the influence of the eccentricity on the horizontal displacements measured at three positions: eccentricity, point *m*, and ground surface. Larger values of horizontal displacements observed in eccentricity curves are essentially due to the deflection of the pile, which is related to its stiffness. However, it is worth emphasizing the need to be more careful with eccentricities above 0.9 m as they present deflections greater than 40 mm. Considering practical application, these values must be lower than those tolerated by the suppliers of the photovoltaic modules. On the other hand, it is possible to observe that the horizontal displacements measured at the ground surface and point *m* are greater than 10 mm for eccentricities above 0.6 m. This observation is important since the eccentricity of 1.2 m is adopted in the design of the tracker

systems. At this eccentricity, it is expected a larger horizontal displacement than that specified for the design load of 11.6 kN. Corroborating the above considerations, Fig. 7b shows the variation of the lateral load with eccentricity for horizontal displacement of 10 mm and 25 mm measured at the ground surface and point *m*. Equations describing the decrease in lateral load with the eccentricity are also shown in the figure. Again, it is possible to clearly observe eccentricities where the applied lateral loads are greater than the design load and increased loads (150% and 250%), for horizontal displacements of 10 mm and 25 mm, respectively. If the same eccentricities and horizontal displacements are considered, it is concluded that point *m* tends to be a more conservative condition to measure horizontal displacement, as it presents lateral loads smaller than the ground surface.

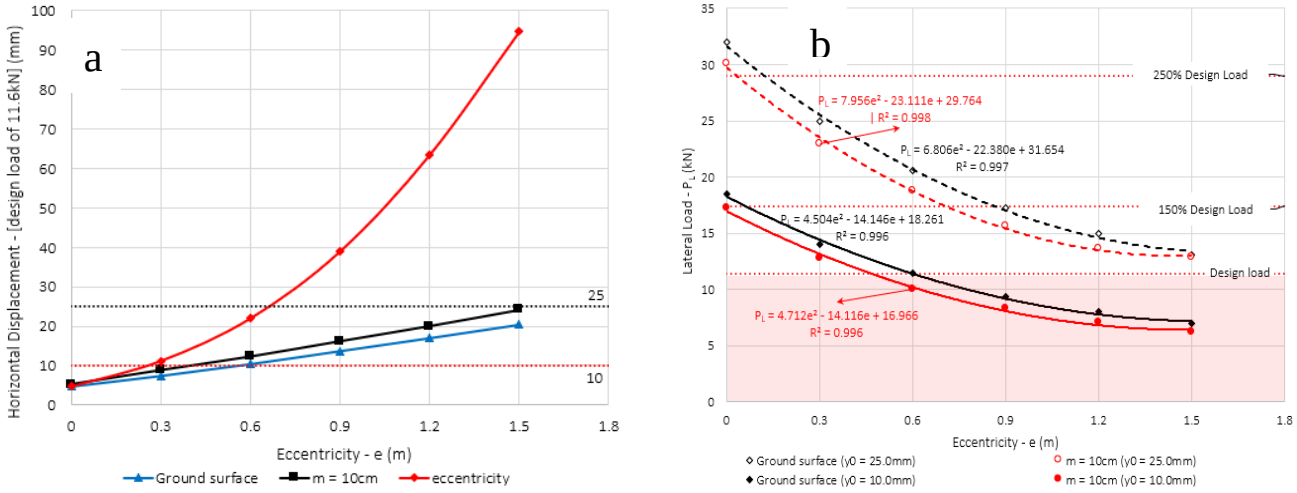

Figure 7. a) variation of the horizontal displacement with eccentricity, and b) variation of the lateral load with eccentricity

A linear increase of y_{res} (difference between horizontal displacements at point m and the ground surface) with the horizontal displacement at point m can be seen in Fig. 8, for different eccentricities. Both Figs. 8a and 8b show that, for the same value of horizontal displacement at point m or ground surface, larger values of y_{res} correspond to larger eccentricities. In Fig. 8a, y_{res} ranges from 1.38 mm to 1.70 mm and ranges from 3.05 mm to 3.75 mm, when displacements at point m are 10 mm and 25 mm, respectively. In Fig. 8b, y_{res} ranges from 1.55 mm to 2.00 mm and ranges from 1.40 mm to 4.40 mm, when displacements at the ground surface are 10 mm and 25 mm, respectively. For analyzes and designs performed based on horizontal displacement at the ground surface, the load-displacement curve measured at point m should be corrected based on the y_{res} presented in Fig. 8a. Again, it is worth mentioning that the magnitudes of the curves presented in this figure depend on the geometry and stiffness of the pile and the soil profile.

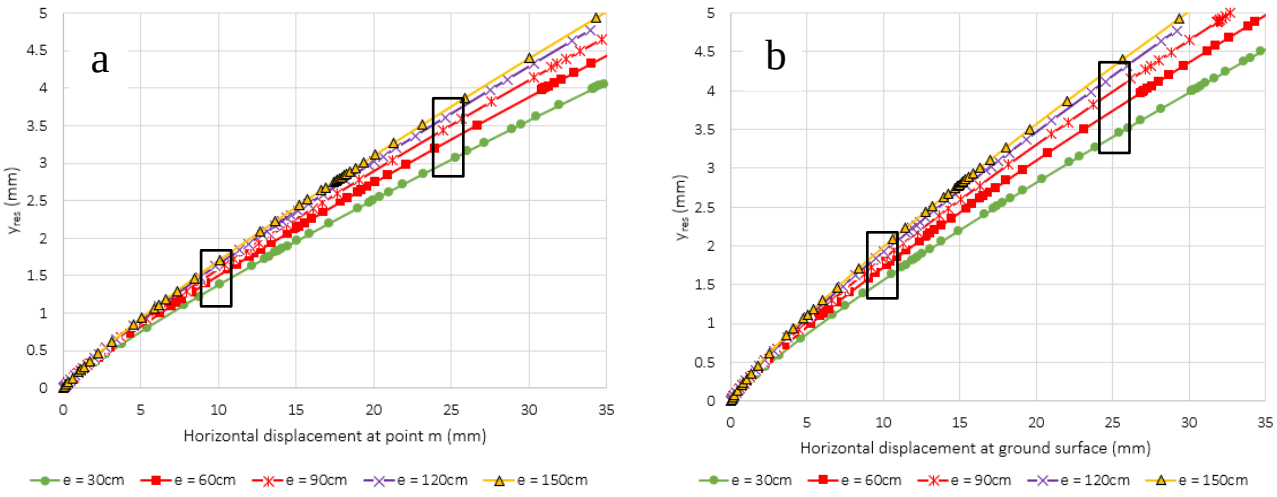

Figure 8. y_{res} *versus* horizontal displacement

Topics, such as cyclic loading, plastification zones and load transfer - of great interest for the understanding

of the interaction mechanism between soil and piles subjected to wind loads are analyzed in other papers part of this research.

5 Conclusions

The effects of eccentricity and displacement measurement points on load-displacement curves measured in laterally loaded piles are investigated numerically using the FE software. For a better understanding of this mechanism, two cases were numerically modeled. As conclusions, the numerical model calibrated based on experimental load tests results seems reliable and presents satisfactory results from a practical point of view. The eccentricity has considerable effects on load-displacement curves. For the same horizontal displacement, lateral loads increase with decreasing eccentricity, while horizontal displacements increase with eccentricity. These behaviors are also dependent on soil and pile characteristics. For a given lateral load, the magnitude of horizontal displacement does not depend only on the factors listed above, but also on the point where the horizontal displacement is measured. Because of this, the load-displacement curves measured at point *m* must be corrected when the analysis and designs consider horizontal displacement at the ground surface. This correction can validate load test results that would fail for excessive horizontal displacement. In addition, it can be concluded that for the same horizontal displacement at point *m*, larger values of y_{res} correspond to larger eccentricities. For practical application, some quantities and considerations about lateral load and horizontal displacements in Serviceability Limit State and Ultimate Limit State are presented and discussed in this work. Although the paper addresses only a part of a larger research, the conclusions presented are of great importance for planning lateral load tests and interpreting their results in solar photovoltaic parks.

Acknowledgements. The authors thank the Federal University of Santa Catarina for the infrastructure and financial support and the SETA-Araxá Consortium for the data and technical support during the development of this research project.

Authorship statement. The authors hereby confirm that they are the sole liable persons responsible for the authorship of this work, and that all material that has been herein included as part of the present paper is either the property (and authorship) of the authors, or has the permission of the owners to be included here.

References

[1] S. Mohapatra, "Wind tunnel investigation of wind load on a ground mounted photovoltaic tracker". 2011, Master thesis, Colorado State University, USA, 2011.
[2] A. M. Silva, "Wind load on solar trackers". 2013, Master thesis, Nova University Lisbon, Portugal. 2013.
[3] B. Kaabia, S. Langlois and F. Légeron, "Full-scale measurement of the response of a CPV tracker structure prototype under wind load". *Solar Energy*, vol. 147, pp. 368–380, 2017.
[4] J. C. Wu, K. H. Lin and C. K. Lin, "Wind Load Analysis of A Solar Tracker For Concentrator Photovoltaics". In: *6th International Conference on Concentrating Photovoltaic System*, Proceedings...pp. 145 -148. . 2010.
[5] N. Aoki, D. A. Velloso, "An Approximate method to estimate the bearing capacity of piles". In: *Panamerican Conference on Soil Mechanics and Foundation Engineering*, Proceedings…Buenos Aires, 1975.
[6] L. Décourt, A. R. Quaresma Filho, "Pile load capacity from SPT values". In *6th Brazilian Congress of Soil Mechanics and Foundation Engineering*, Proceedings… Rio de Janeiro, Vol. 1, pp. 45-53, 1978.
[7] L. C. Reese, W. R. Cox and F. D. Koop, "Analysis of Laterally Loaded Piles in Sand". In *Offshore Technology Conference*, Proceedings…Texas, 1974.
[8] B. B. Broms, "Lateral resistance of piles in cohesive soils". *Journal of the Soil Mechanics and Foundation Division*, American Society of Civil Engineers, vol .89, pp. 27-63, 1964.
[9] B. B. Broms, "Lateral resistance of piles in cohesionless soils". *Journal of the Soil Mechanics and Foundation Division*, American Society of Civil Engineers, vol. 89, pp. 123-157, 1964.
[10] H. Matlock, and L. C. Reese, "Generalised solutions for laterally loaded piles". *J. Soil Mech. Found. Div*., vol. 86, pp. 91-97, 1960.
[11] C. S. Desai, G. C. Appel, "3-D analysis of laterally loaded structures". *Second International Journal Conference on Numerical Methods in Geomechanics*, pp. 405–418, 1976.
[12] C. S. Desai, T. Kuppusamy, "Application of a numerical procedure for laterally loaded structures". *Numerical Methods in Offshore Piling*, pp. 93–99, 1980.
[13] Y. Khodair and A. A. Mohti, "Numerical analysis of pile-soil interaction under axial and lateral loads". *International Journal of Concrete Structures and Materials*, vol. 8, pp. 239 – 249, 2014.